THE USE AND IMPLEMENTATION OF DYNAMICAL CLOUD MODELS IN A PARAMETRISATION SCHEME FOR DEEP CONVECTION

M.J.Miller* and M.W. Moncrieff
Atmospheric Physics Group
Imperial College, London, U.K.

1. INTRODUCTION

The convective transport of heat is an important mechanism for generating available potential energy for the large-scale systems which are vital for determining the nature of the general circulation of the atmosphere. However, the dynamics of the synoptic-scale weather systems in the tropics are more directly affected by deep convection. The role of the convective transport of dynamical properties, such as horizontal momentum, is a much more subtle consideration and the nature of this process is not well understood. Present parametrisation schemes do not treat the transport of heat and momentum in a consistent fashion, and cloud dynamics are not represented despite many types of deep convective clouds being dynamically controlled and organised. Indeed, cloud models are either absent from present parametrisation schemes or are very simple.

It is conceivable that future general circulation models will require a more realistic representation of convective dynamics as grid (or spectral) resolution converges on the potential energy producing scales of motion. Indeed, the horizontal scales of organised systems of convection, e.g. squall lines, cloud clusters and mesoscale complexes are already comparable to existing grid-scales.

---

*Currently at the European Centre for Medium Range Weather Forecasts.

This paper will consider only deep convective systems, in particular those which are associated with precipitation, downdraughts and a degree of flow organisation. (Shallow convection has an important though separate role to play in the heat transport problem). A number of different types of cloud model will be presented and an important aspect is the consistent treatment of thermodynamical and dynamical quantities. These models are of a semi-analytic nature and are novel because they can be directly used in existing methods for linking sub-grid-scale and grid-scale variables. The relevance of dynamical models is therefore being tested in present parametrisation methods, and for this purpose the models are kept as simple as possible.

The earlier sections of this paper establish the theoretical framework of the cloud models and their incorporation into a parametrisation scheme, and results of tests of the scheme in simplified and full global forecasts are then discussed.

2. OBSERVED TYPES OF ORGANISATION IN DEEP CONVECTION

The combined effects of vertical wind shear, convective available potential energy and evaporative-driven downdraughts can organise and control the dynamics of deep convection. It has long been known that vertical shear is important in determining the structure and travel speed of mid-latitude squall-lines and storms. For instance, Browning and Ludlam (1962), Newton (1966)and Marwitz (1972) all show different aspects of the structure of mid-latitude convective squall-lines and cumulumbus. The dynamical structure of the tropical squall line, as in Zipser (1969), Houze (1977) and extensively reviewed in Houze and Betts (1981), is shown to be quite different from the mid-latitude type. Instead of travelling with a mid-level wind velocity, as is typical of mid-latitude systems, tropical systems tend to propagate relative to the winds at all levels. This radically changes the nature of

the relative flow in these two cases, a property which will be considered later. The processing of mass, energy and momentum is therefore fundamentally different in these two types of convection. Although a single system may involve a number of transient convection cells, there is frequently a quasi-steadiness or persistence of the system as a whole. The occurrence of these types of convection is closely associated with forms of the wind profile, and in particular the vertical shear.

In the case where the vertical wind shear is small, the convection is organised in a different sense. Instead of travelling over large distances without significant change of form, the convection consists of three distinct phases, an udpraught (growing) phase, a mature phase and a downdraught (dissipating) phase. This is typified in the study of Byers and Braham (1949), and is probably the most prevalent type of deep convection, and so has to be included in a dynamical representation of deep convection.

3. A DYNAMICAL CLASSIFICATION OF DEEP CONVECTION SUITABLE FOR PARAMETRISATION

The dynamical structure of convection in a sheared flow is complex and in order to facilitate progress, basic assumptions have to be made. The classification of convection into dynamical types is a particularly useful concept. Previous dynamical analysis reviewed by Moncrieff (1981) suggests that convection models can, at least for parametrisation purposes, be classified into a number of distinct types. Four types are of particular interest, namely, Classical, Steering-level, Propagating and Jump models, and these are shown in Fig.1.

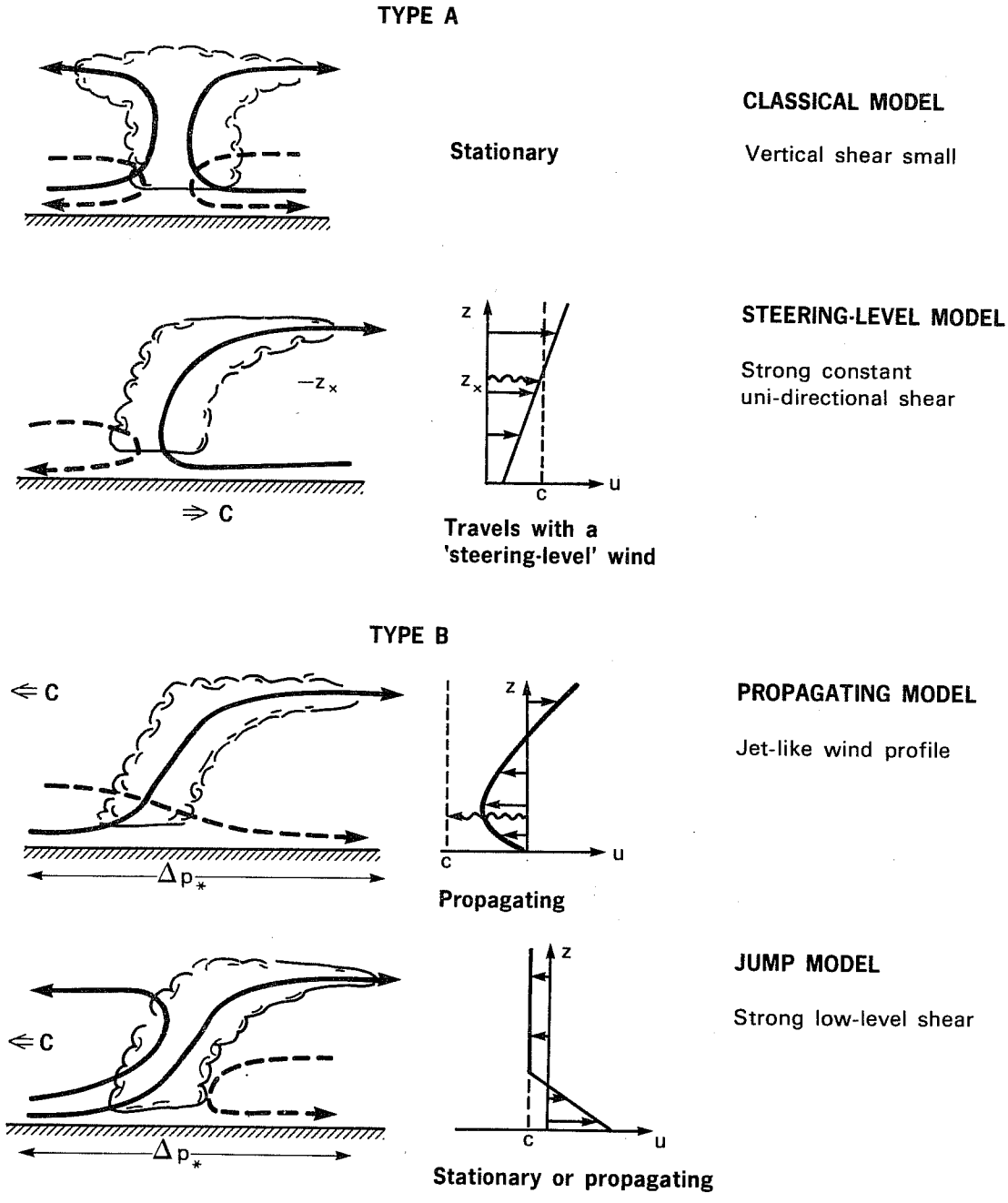

Fig. 1 Schema of dynamically distinctive types of organised convection of particular relevance to parametric representation.

4. THEORETICAL BASIS

Details of the theoretical basis for the convection models can be found in a series of papers: Moncrieff and Green (1972), Moncrieff and Miller (1976), Moncrieff (1978, 1981), Thorpe, Miller and Moncrieff (1980, 1982), so only significant points will be considered here. Height is used as the vertical coordinate throughout, since in this case some particularly useful exact conservative properties can be obtained. Since the macro-scale motion is of primary importance, it is convenient to neglect small scale effects, and so inviscid equations are assumed.

4.1 Momentum

The non-hydrostatic, quasi-Boussinesq equations are used with perturbations of pressure and potential temperature, δp, $\delta\theta$ from a static state p_o, θ_o

$$\frac{D\underset{\sim}{v}}{Dt} + \nabla\left(\frac{\delta p}{p_o}\right) - g\,\frac{\delta\theta}{\theta_o}\,\underset{\sim}{k} = 0$$

4.2 Thermodynamics

In deep convection, the heating/cooling rate (Q/C_pT) following a particle is mainly latent heating/evaporative cooling, in which case the wet-bulb potential temperature (or equivalent potential temperature) is conserved. Therefore, since $\frac{d}{dz}(\ln q_s) >> (\ln T)$, and $\theta = \theta_o + \delta\theta$

$$\frac{D}{Dt}(\ln\theta) = \frac{Q}{C_pT} \simeq -\,w\,\frac{L}{C_p}\,\frac{dq_s}{dz} = w\Gamma$$

and so

$$\frac{D}{Dt}\left(\frac{\delta\theta}{\theta_o}\right) = w(\Gamma - B)$$

where $B = \frac{d}{dz}(\ln\theta_o)$ is the undisturbed static stability. It follows by using

the Fundamental Theorem of calculus applied to total derivatives that,

$$\frac{D}{Dt}\left(\frac{\delta\theta}{\theta_o} - \int_{z_o}^{z} (\Gamma - B)dz\right) = 0$$

where $z - z_o$ is a particle displacement along a trajectory with inflow height $z = z_o$. If no perturbations exist on inflow, then

$$\frac{\delta\theta}{\theta_o} = \int_{z_o}^{z} (\Gamma - B)dz \qquad (1)$$

So $\frac{\delta\theta}{\theta_o}$ along a particle path is given by the integrated difference between particle and environment lapse rates.

4.3 Mass

The mass continuity equation in a quasi-Boussinesq system is given by

$$\mathrm{div}(\rho \underset{\sim}{v}) = 0$$

When integrated over a streamtube volume, Gauss' Theorem equates the outflow mass flux and the inflow mass flux,

$$\rho_1 \left|\underset{\sim}{v}_1\right| dy_1 dz_1 = \rho_o \left|\underset{\sim}{v}_o\right| dy_o dz_o \text{ and}$$

$$\left|\underset{\sim}{v}_1\right| = \left(\frac{\rho_o}{\rho_1}\frac{dy_o}{dy_1}\frac{dz_o}{dz_1}\right)\left|\underset{\sim}{v}_o\right| \qquad (2)$$

where $dy_o dz_o$ and $dy_1 dz_1$ are respectively the inflow and outflow cross-sections of this streamtube, with inflow height $z = z_o$ and outflow height $z = z_1$. Therefore the outflow speed $\left|\underset{\sim}{v}_1\right|$ can be obtained in terms of the inflow speed provided the displacement of particles is known.

4.4 Energy

Operating $\underset{\sim}{v}$. on the momentum equation gives the energy equation per unit mass:

$$\frac{D}{Dt}\left(\tfrac{1}{2}\underset{\sim}{v}^2\right) + \underset{\sim}{v}\cdot\nabla\left(\frac{\delta p}{\rho_o}\right) - g\,\frac{\delta\theta}{\theta_o}\,w = 0$$

Assuming steady flow ($\partial/\partial t = 0$) in a frame of reference moving at the travel speed of the system,

$$\frac{D}{Dt}\left(\tfrac{1}{2}\underset{\sim}{v}^2 + \frac{\delta p}{\rho_o} - \int_{z_o}^{z} g\,\frac{\delta\theta}{\theta_o}\,dz\right) = 0$$

so the particle kinetic energy per unit mass ($\tfrac{1}{2}\underset{\sim}{v}^2$) measured along a streamline is given by

$$\tfrac{1}{2}\underset{\sim}{v}^2 = \tfrac{1}{2}\underset{\sim}{v}_o^2 - \frac{\delta p}{\rho_o} + \int_{z_o}^{z} g\,\frac{\delta\theta}{\theta_o}\,dz\ , \qquad (3)$$

the sum of the inflow specific kinetic energy, the work done by buoyancy (equal to the convective available potential energy) and the work done by pressure along a streamline.

4.5 Particle displacement equation

The above equations arise from a Lagrangian representation, so the particle displacement is a basic dependent variable. Clearly Eqs. (1,3) can be combined to give

$$\tfrac{1}{2}\underset{\sim}{v}^2 = \tfrac{1}{2}\underset{\sim}{v}_o^2 - \frac{\delta p}{\rho_o} + \int_{z_o}^{z}\int_{z'_o}^{z'} g\,(\Gamma - B)\,dz'dz \qquad (4)$$

Applying Eq.(4) to outflow and referring to Fig.2, if $z = z_1$ is the outflow height of the streamline having inflow height $z = z_o(z_1)$, and if the outflow pressure is hydrostatic

$$\left(\frac{\delta p}{\rho}\right)_1 = \left(\frac{\Delta p}{\rho}\right)_* + \int_{z_*}^{z_1} g\,\left(\frac{\delta\theta}{\theta}\right)_1 dz_1 \qquad (5)$$

it follows that on outflow

$$\tfrac{1}{2}\underset{\sim}{v}_1^2 = \tfrac{1}{2}\underset{\sim}{v}_o^2 - (\frac{\Delta p}{\rho})_* - \int_{z_*}^{z_1}\int_{z_o'}^{z_1'} g\,(\Gamma - B)dz_1'dz_1 + \int_{z_o}^{z_1}\int_{z_o'}^{z'} g\,(\Gamma - B)dz'dz$$

where subscripts (o) and (1) refer to inflow and outflow of the same streamline. Using Eq.(2), it follows that

$$\tfrac{1}{2}\left(\frac{\rho_o}{\rho_1}\frac{dy_o}{dy_1}\frac{dz_o}{dz_1}\right)^2 \underset{\sim}{v}_o^2 = \tfrac{1}{2}\underset{\sim}{v}_o^2 - (\frac{\Delta p}{\rho})_* - \int_{z_*}^{z_1}\int_{z_o'}^{z_1'} g\,(\Gamma - B)dz_1'dz_1$$

$$+ \int_{z_o}^{z_1}\int_{z_o'}^{z'} g\,(\Gamma - B)dz'dz \qquad (6)$$

This equation is very general, since the inflow $\underset{\sim}{v}_o$ and the lapse rates Γ and B can be any specific functions; the only necessary constraints are that the flow should be steady and the heating/cooling rates should be proportional to the vertical velocity. For application to cloud models, however, this generality at present gives unnecessary complication. In certain special cases analytic solutions are possible and assumptions can be made which simplify the problem considerably:

(a) $\Gamma = \gamma$ and B are constant lapse rates

(b) $dy_o = dy_1$ and $\underset{\sim}{v} = u(z)\underset{\sim}{i}$ a two-dimensional outflow/inflow approximation.

(c) $\rho_o = \rho_1$, constant density.

With these simplifications, Eq.(6) reduces to

$$\left(\frac{dz_o}{dz_1}\right)^2 = 1 - \frac{\Delta p_*}{\frac{1}{2}\rho u_o^2} + \frac{g(\gamma-B)}{\frac{1}{2}u_o^2}\left[\frac{(z_1-z_o)^2}{2} - \int_{z_*}^{z_1}(z_1-z_o)dz_1\right] \qquad (7)$$

This particle displacement holds everywhere except at inflow stagnation points ($u_o = 0$) and it is the fundamental equation for the system. In applying the models in a parametrisation scheme, however, non-constant density has to be allowed for by modifying the solutions. This is not difficult to achieve and leads to approximate, rather than exact, solutions.

4.6 Basic types of model

The solutions of Eq.(7) represent two distinctive types of relative flow associated with the type A and type B classification of Sect.2. These are distinguished in Fig.2 and the basic difference lies in the form of the streamlines and the dynamical pressure term Δp_*, which is the inflow/outflow pressure change along a streamline having inflow height $z = z_*$. In type 'A', this streamline limits to a stagnation point and since pressure must be continuous in a fluid $\Delta p_* = 0$. On the other hand, in type 'B', this streamline is displaced to the outflow side of the system and clearly there is no such constraint on Δp_*, so in general $\Delta p_* \neq 0$. The first type of solution is relevant to the classical steering level models considered in Moncrieff and Green (1972), Moncrieff (1978, 1981), whereas the second was considered in the propagating and jump models of Moncrieff and Miller (1976) and Thorpe, Miller and Moncrieff (1980, 1982).

The distinction between these two basic types has fundamental implications regarding momentum parametrisation, since the pressure field is a potential source of momentum, in addition to that available from the buoyancy field.

5. CALCULATION OF CONVECTIVE FLUXES FROM THE STEADY MODELS

A method of incorporating convective fluxes into large-scale models is presented in Ooyama (1971) and Fraedrich (1973) and this is the approach followed. If no storage is assumed, then the contribution of the convective fluxes to the grid-scale equation is due to two processes, lateral fluxes and vertical fluxes. If ϕ is any scalar variable then these fluxes are, in height coordinates,

$$Q_\phi(z) = \frac{a}{A}\left[\delta\phi \frac{\partial}{\partial x}(\delta u_c) + w_c \frac{\partial \bar{\phi}}{\partial z}\right] \tag{8}$$

where a/A is the fractional area occupied by the convection, $\delta u_c = u_o$ on inflow and $\delta u_c = u_1$ on outflow. The models considered here are two-dimensional and the net effect of deep convection is represented by a single convective circulation, so in this case referring to Fig.3, $a/A \equiv L_c/L$. If Eq.(8) is interpreted in terms of an environment response, further simplifications can be made. In general, the cloud and environment mass fluxes are not simply related. However, if the assumption is made that the convective mass flux through the sides of a grid volume is zero, the problem is somewhat simpler: $w_c L_c = -(L - L_c)w_e$ and if in addition $L_c/L \ll 1$, $w_c L_c = -Lw_e$. Moreover it follows that

$$\frac{L_c}{L}\frac{\partial}{\partial x}(\delta u_c) = -\frac{\partial}{\partial x}(\delta u_e) \simeq \frac{\delta u_c}{L/2}$$

and Eq. (8) can be written in terms of the environment approximately as

$$Q_\phi(z) \simeq 2\delta\phi \frac{\delta u_c}{L} - w_e \frac{\partial \bar{\phi}}{\partial z} \tag{9}$$

The terms on the right-hand side of Eq.(9) represent lateral fluxes of ϕ into the environment and the effect of environmental subsidence on the mean profile ϕ.

A

'STEERING-LEVEL' RELATIVE FLOW CONFIGURATION

e.g. Classical and steering-level models

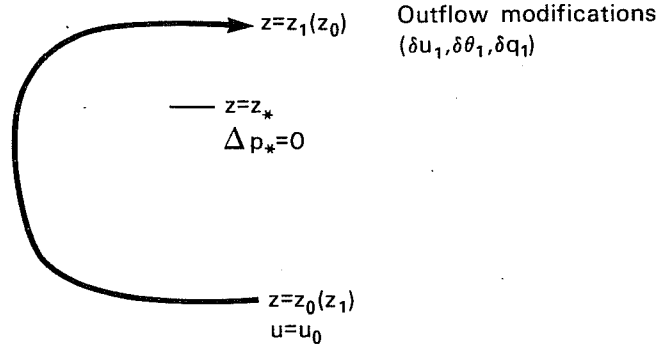

B

'PROPAGATING' RELATIVE FLOW CONFIGURATION

e.g. Propagating and jump models

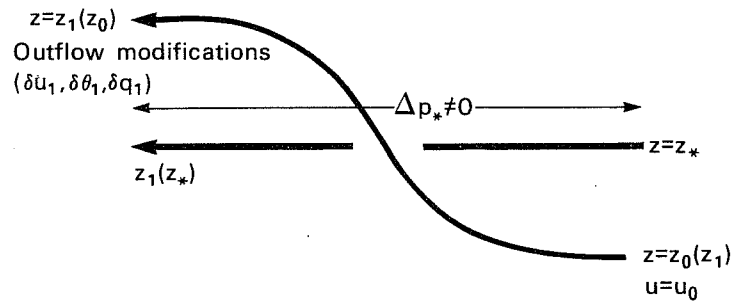

$$\delta u_1 = u_0(z_0)\frac{dz_0}{dz_1} \; ; \; \left(\frac{\delta\theta}{\theta}\right)_1 = (\gamma - B)(z_1 - z_0) \; ; \; \delta q_1 = q_s(T_1) - \bar{q}(z_1, \bar{T})$$

Fig. 2 Schema of two basic types of relative flow, showing the distinction between $\Delta p_*=0$ and $\Delta p_*\neq 0$, in terms of streamline configuration.

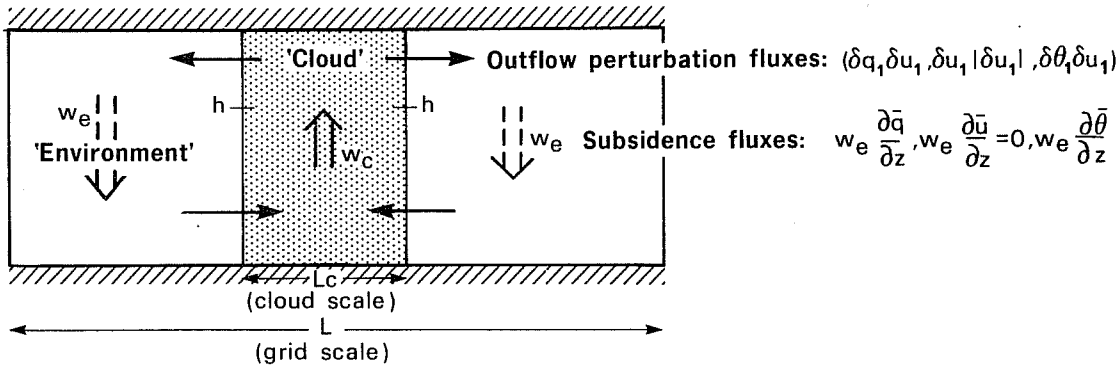

Fig. 3 Schematic diagram showing outflow fluxes and environment subsidence.

5.1 Determination of the outflow fluxes from the steady model solutions

Once the solutions $z_o(z_1)$ and $z_1(z_o)$ to the displacement equation have been found then the relative outflow changes can be calculated:

(a) The outflow potential temperature change $\delta\theta_1$ is given by Eq.(1), which in the particular case of Γ, B constant gives

$$\left(\frac{\delta\theta}{\theta}\right)_1 = (\Gamma - B)(z_1 - z_o) \tag{10}$$

(b) The relative outflow speed (u_1) is given by Eq.(2), which in the special case of $\rho_o = \rho_1$, $dy_o = dy_1$ etc. reduces to

$$\delta u_1 = u_1 = u_o \frac{dz_o}{dz_1} \tag{11}$$

(c) The change in specific humidity can be determined if the outflow is assumed to be saturated. If the overbar denotes the grid scale quantities, then

$$\delta q_1(z_1) = q_s(T_1) - \bar{q}\ (z_1, \bar{T}) \tag{12}$$

where $T_1(z_1) = \bar{T}(z_1) + \delta T_1$ with δT_1 obtained from $(\delta\theta/\theta)_1$ by using the second law of thermodynamics and Eq.(5).

The Eqs.(10,11,12) allow the relative outflow fluxes to be obtained directly per unit mass:

$$\begin{aligned} &\text{outflow sensible heat flux} && = C_p\ \delta T_1\ \delta u_1 \\ &\text{outflow latent heat flux} && = L\ \delta q_1\ \delta u_1 \\ &\text{outflow momentum flux} && = \left|\delta u_1\right|\ \delta u_1 \end{aligned} \tag{13}$$

5.2 Determination of the vertical fluxes from model solutions

Since the cloud model solutions give the inflow/outflow speeds $\delta u_c(z)$ it follows that w_c (or w_e) can be obtained directly by integrating the cloud scale mass continuity equation $\frac{\partial}{\partial x}\ (\delta u_c) + \frac{1}{\rho}\frac{\partial}{\partial z}\ (\rho w_c) = 0$ giving

$$w_c(z) = -\frac{1}{\rho} \int_o^z \rho\ \frac{\partial}{\partial x}\ (\delta u_c)\ dz \tag{14}$$

It follows that the terms in Eq.(9) can be directly calculated from the cloud models, and this is a novelty of this type of dynamical approach to the parametrisation problem. Although these dynamical models are much simpler than in reality, they are thermodynamically and dynamically consistent and are at any rate more flexible than those previously used in parametrisation schemes, especially since more than one regime of convection can be represented.

6. AN EXAMPLE - THE CLASSICAL MODEL

This is the simplest type of dynamical model which is considered in this approach, consisting of updraught and downdraught circulations as shown in Fig.4. In fact, the system can be considered as having four different branches, namely a pair of updraughts and a pair of downdraughts. These branches of flow are similar and it is sufficient to consider the updraught circulation branch as shown in Fig.4. It is important to note that the inflow to this system is that induced by the convection.

If the inflow is assumed to have constant inflow shear $du_o/dz_o = A$ then the asymptotic solution of Moncrieff and Green (1972) can be applied to this model. The displacement equation in this case is

$$\left(\frac{dz_o}{dz_1}\right)^2 = 1 + \frac{4R_u}{(z_o - h)^2}\left[\frac{(z_1 - z_o)^2}{2} - \int_h^{z_1} (z_1 - z_o)dz_1\right]$$

where $R_u = UCAPE/\frac{1}{2}(AH)^2$ and $UCAPE = \frac{1}{2}g(\gamma-B)H^2$ is the convective available potential energy for the updraught parcel originating at $z_o = 0$. The value of the Richardson Number (R_u) determines h/H and $z_o(z_1)$, representing an eigenvalue and eigensolution. In this case of constant inflow shear an analytic solution to the displacement equation exists and is

$$h = H(1 + \sqrt{1 + 4\,R_u})/(3 + \sqrt{1 + 4\,R_u})$$

$$z_1(z_o) = h + \frac{2(h - z_o)}{(1 + \sqrt{1+4R_u})}$$

Using the equation for the outflow modification Eqs.(10,11,12) it is easily shown that

$$\delta u_1(z_1) = \frac{1}{2H}\sqrt{\frac{2UCAPE}{R_u}}\,(1 + 2\,R_u + \sqrt{1 + 4\,R_u})(z_1 - h)$$

$$(\frac{\delta\theta}{\theta})_1(z_1) = \frac{UCAPE}{gH^2}\,(3 + \sqrt{1 + 4\,R_u})(z_1 - h)$$

$$\delta q_1(z_1) = q_s(T_1) - \bar{q}(z_1,\bar{T})$$

where the overbar denotes the gridscale quantities, and from these the updraught outflow fluxes can be determined, as in Eq.(13).

Using Eq.(14) the horizontally averaged updraught speed can be calculated:

$$w_c(z) = \begin{cases} \frac{H}{L_c}\sqrt{\frac{2UCAPE}{R_u}}\,\frac{z}{H}\,(\frac{2z}{H} - \frac{h}{H}) & 0 \leq z \leq h \\ \frac{H}{L_c}\sqrt{\frac{2UCAPE}{R_u}}\,(\frac{1 + 2\,R_u + \sqrt{1 + 4\,R_u}}{5 + 2\,R_u + 3\sqrt{1 + 4\,R_u}})\left[1 - (\frac{z-h}{H-h})^2\right] & h \leq z \leq H \end{cases} \qquad (15)$$

Consequently the flux divergences of sensible heat, latent heat and momentum $C_pQ_T^u$, LQ_q^u and Q^u due to the updraught can be found:

$$Q_T^u(z) = \frac{2\delta u_1 \delta T_1}{L} - w_e(\frac{\partial\bar{T}}{\partial z} - \frac{g}{c_p})$$

$$Q_q^u(z) = \frac{2\delta u_1 \delta q_1}{L} - w_e\frac{\partial\bar{q}}{\partial z}$$

$$Q_m^u(z) = 0$$

The factor of two in the outflow fluxes arises because there are two updraught branches.

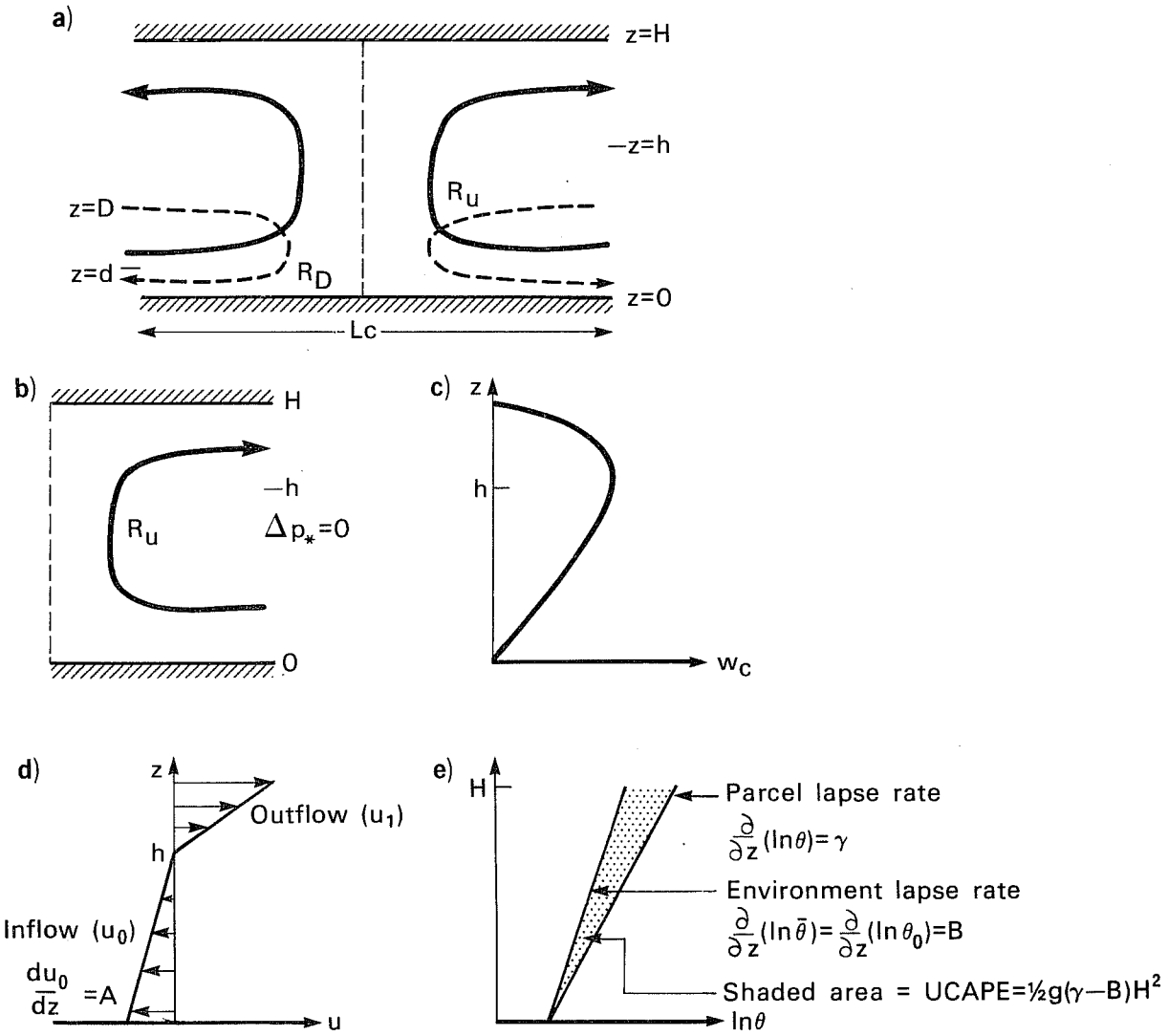

Fig. 4 Schematic representation of the classical model. a) Flow configuration b) Typical updraught branch with $R_u=\frac{UCAPE}{1/2(AH)^2}$, $\Delta p_*=0$ c) Mean updraught speed W_c (see Eq. (12)) d) Inflow/outflow speeds from displacement solutions e) Parcel $\ln\theta$ for special case of parcel originating at $z_0=0$ and outflowing at $z_1=H$ so UCAPE=1/2 g(γ - B)H^2.

The inverse dependence of both terms in $Q_{T,q}$ on the gridscale L emphasises the problem of parametrisation as the gridscale converges on the scales of the processes to be parametrised.

Flux divergences for the downdraught branches of the circulation can be found in a similar manner.

7. MOMENTUM TRANSPORT

Heat transports by different types of steady model are broadly similar and typified by middle and upper-level warming by the updraught outflow and subsidence response and low-level cooling by the downdraught. The momentum transports can, however, be markedly different, the form of the transport depending on the type of model. The momentum transport will only be summarised here, and the details can be found in appropriate publictions.

Due to the vertical symmetry of the flow and the pressure field the classical model does not transport momentum; it is therefore a special case.

The steering-level model has an asymmetry imposed by the vertical shear and, in this case, the cloud scale momentum transport is counter-gradient - see Moncrieff and Green (1972), and Moncrieff (1978, 1981). Moreover, in the parametrisation context, there is a net momentum generation in a grid-volume because although the vertical flux convergence $\partial/\partial z(w_c \bar{u})$ integrates to zero, the lateral flux term $u_c \, \partial u_c/\partial x$ provided a net source of momentum.

The propagating model has a different type of transport. It is shown in Moncrieff and Miller (1976), Moncrieff (1981) that this model typically causes relative outflow stagnation in mid-levels, but the lower and upper level flow is enhanced. The result is that a "jet like" outflow profile is established.

Since this type of convection is associated with jet-like inflow profiles (reverse shear) in tropical regions, this means that the cloud-scale outflows enhance the jet.

The jump model is again quite different, and is associated with mean flow which has a strong low-level shear (Thorpe, Miller and Moncrieff (1982)). Moreover, the downdraught is relatively weak with the result that the main feature of the momentum transport is that the low-level flow is 'blocked', leading to significant momentum transport in low-levels. Since the upper level flow can split into two branches, the net effect on the upper level flow is not as marked.

In the propagating and jump models, the work done by the pressure field along streamlines is important, and this highlights the difference between the type 'A' and type 'B' models previously discussed.

Although the outflow momentum fluxes are quite distinctive, the subsidence fluxes are more easily interpreted because the subsidence term simply effects a downward advection of the mean wind profile.

Since the models described here are two-dimensional, the momentum transports do not generate a sub-grid-scale vertical vorticity transport, However, grid-scale vertical vorticity transport exists because adjacent grid-volumes are affected differently. There are, however, substantial horizontal vorticity transports, which are more important on the cloud scale, mainly because vertical shear is usually an order of magnitude larger than the horizontal shear.

8. MESOSCALE ORGANISATION OF CONVECTION

In certain cases convection is organised on a mesoscale, for example in squall-lines, convective complexes and clusters, and the scale of these systems is comparable to the grid-scale in present models. Some of these phenomena will be partially resolved by future general circulation models, and it is even possible that these could be explicitly treated. At least a different treatment from present parametrisation methods will be required because these methods represent systems which are much smaller than the grid scale. Little is known of the significance of such a distinction in the scale of the system being parametrised. However, in the case of the tropical squall line, it is clear that mesoscale ascent and descent can be forced by the cloud scale transports. Moreover, in this case the heat transports associated with the mesoscale organisation are completely different from those occurring on the cloud scale, and the momentum transport is even more distinctive.

It is envisaged that the approach considered here is capable of representing certain mesoscale systems and in this sense it has a significant generality. However, this aspect requires much more research before quantitative statements can be made on the distinction between cloud and mesoscale convective parametrisation.

9. THE IMPLEMENTATION AND TESTS OF THE DEEP CONVECTION SCHEME

The preceding analysis and discussion provides the basis for a parametrisation scheme which has been developed, implemented and tested in the ECMWF gridpoint model. The following sections will demonstrate the viability of this scheme and discuss a number of problems and possibilities for the future. As given in Sect.6 the cloud models provide convective fluxes which can be written in a general form

$$Q_\phi = Q_\phi \left(\text{CAPE, H, shear, } \frac{d\bar{\phi}}{d\sigma}, \text{ L}\right)$$

(where $\phi \equiv$ T, q, u, v) with corresponding downdraught equivalents.

Each of these parameters is readily calculated from the gridscale variables, in particular

$$\text{CAPE} = -R \int_1^{\sigma(H)} (T_p - \bar{T}) \frac{d\sigma}{\sigma}$$

(here expressed using σ as vertical coordinate) and H are calculated by determining a pseudo-adiabatic parcel value T_p from the gridpoint boundary layer parameters and defining H as the level of zero buoyancy. Calculations of downdraught CAPE and depth are more complex and will not be described here.

10. SINGLE-COLUMN MODEL TESTS

The parametrisation scheme incorporates several cloud models (see Sect.3), but for the purpose of testing the basic ideas only, tests of the 'classical' model will be described. It is essential that an understanding of a scheme is obtained in circumstances where some control is available over other physical processes. Consequently, tests were made in a single-column version of the ECMWF gridpoint model in which all large-scale advective and radiative changes were specified from a data set for a 3-day period during Phase III of the GATE describing a composite easterly wave (Thompson, Reed and Recker. 1979); the boundary layer fluxes of heat and moisture were either specified or evaluated using the numerical models boundary layer scheme (Louis et al. 1982). Many simulations have been performed to evaluate the sensitivity of the scheme but only selected results showing the scheme's basic behaviour are given here.

It is characteristic of the tropical atmosphere that the thermodynamic structure changes only slowly, and during the passage of an easterly wave, moisture convergence and adiabatic cooling (up to 10°K/day) are counterbalanced by convective drying and heating by cumulonimbus precipitation; simultaneously the input of heat and moisture from the ocean surface is counterbalanced by downdraughts of lower θ_e. The maintenance of a reasonable vertical temperature and moisture structure is thus a stiff test for a convection scheme.

Fig.5 compares the Miller-Moncrieff scheme (MM) with the Kuo scheme (1974) and Arakawa-Schubert (AS) scheme (1974) against the observed sounding after 80 hours of forecast in which all other processes are specified. It is clear that both AS and MM produce reasonable soundings whereas the Kuo scheme does not. (The Kuo scheme used here is the form in operational use at ECMWF at the end of 1983, it is not the later improved version). Deficiencies in MM are a somewhat too stable and dry lower troposphere and a slightly too moist upper troposphere. The temporal behaviour resulting in this final profile is shown in Fig.6 in which the evolution of equivalent potential temperature during the three-day integration is compared with the observation. Both the vertical and temporal structure of the MM scheme are much smoother than AS.

In practice a convection scheme has to work in conjunction with other model determined processes, and Fig.7 shows the effect on the modelled profile (MM) when the boundary layer scheme is used to determine the surface and low-level vertical fluxes; AS and Kuo also show the cooling of the profile during the forecast. There is a corresponding reduction in convective precipitation and the surface fluxes are only 60% of the values used in the specified experiments. Boundary layer parametrisations are generally developed and tested against fair-weather boundary layer data and it is possible that such

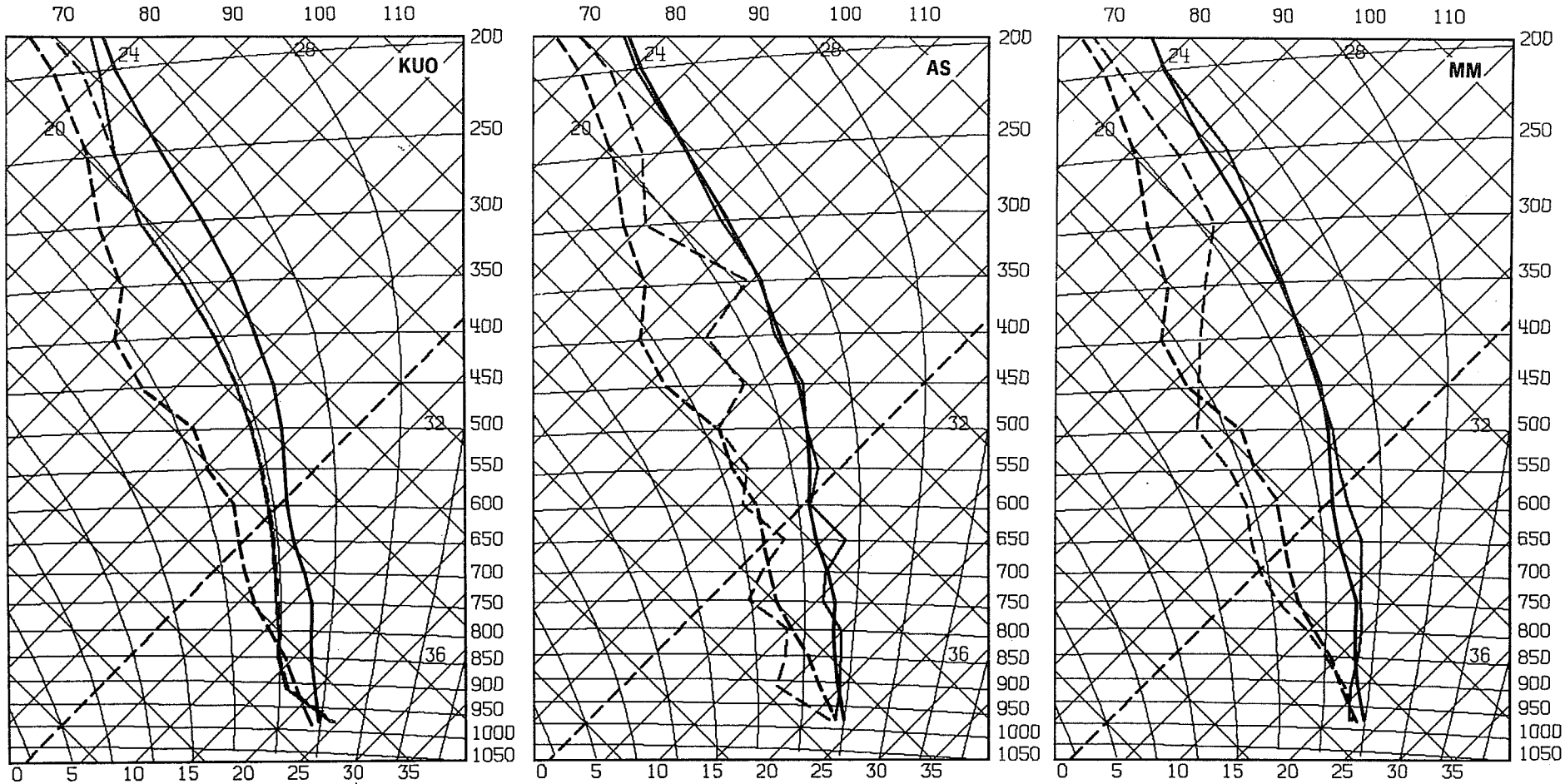

Fig. 5 A comparison of the forecast thermodynamic soundings at 80 hours with that observed. All large-scale and boundary-layer fluxes were specified.

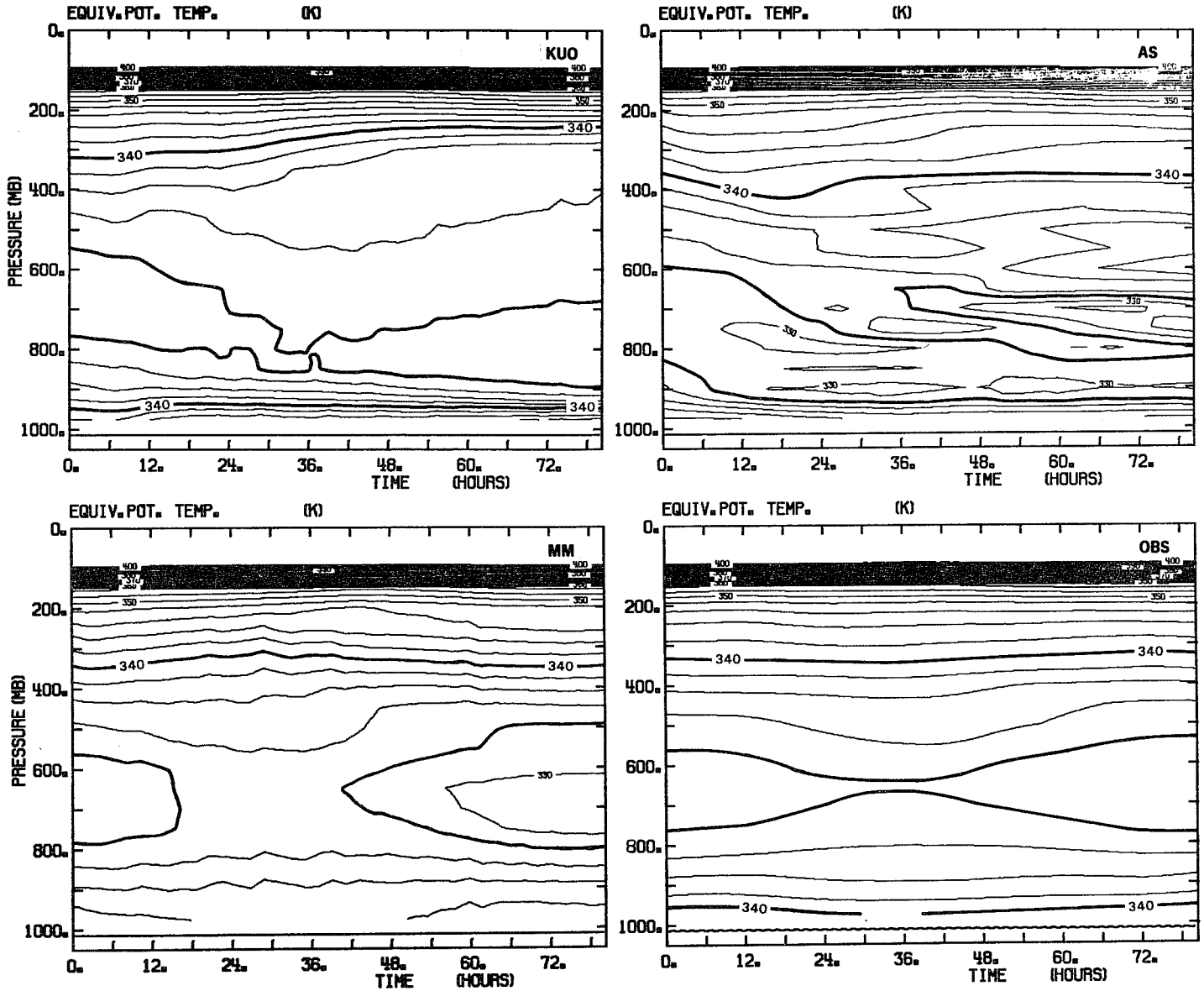

Fig. 6 A comparison of the time-height structure of equivalent potential temperature during the same integrations as in Fig. 5. (Note: θ_E computed from the approximate form $\theta_E = \theta(1+Lq/C_pT)$).

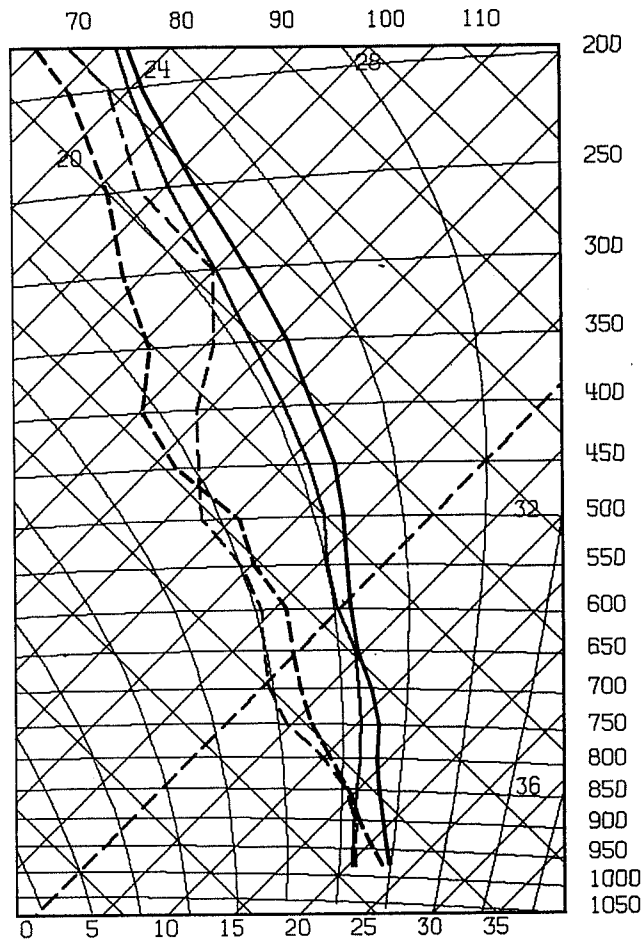

Fig. 7 The predicted and observed sounding at 80 hrs when the boundary-layer fluxes are predicted by the model.

parametrisations are deficient in the highly-disturbed conditions prevalent in the GATE wave data. As a sensitivity test the surface flux calculations were enhanced to near the observed values and results very similar to Fig.5 were obtained. It seems reasonable to expect greatly enhanced fluxes in regions where there are vigorous interactions between downdraught outflows from precipitating clouds and the near-surface layers, and to link the boundary-layer and convection schemes directly may be necessary to properly model the global surface fluxes.

11. GLOBAL MODEL TESTS

11.1 CAPE analysis

When the MM scheme (classical only) was incorporated in a global model forecast a problem immediately arose involving the thermodynamic structure of the initial data. Values of CAPE (see Sect.9) in excess of 3000 J/Kg were typical over substantial regions of the tropics and smaller areas with between 5000 and 10,000 J/Kg. Such high CAPE values are not observed and are a product of the model analysis procedures. Figs.8 and 9 show typical CAPE fields for northern hemisphere winter; Fig.8 a FGGE analysis and Fig.9 a very recent analysis showing some improvement. Fig.10 shows the CAPE field at Day 5 of a forecast using the Kuo scheme and based on the Fig.8 data. Because of the moisture convergence criterion in the Kuo scheme this field does not represent instantaneous convective activity. The maintenance of large CAPE values (Fig.10) can be partly explained by the insensitivity of the Kuo scheme to the magnitude of CAPE; whereas the convective activity for both the MM and AS schemes is directly related to CAPE, this is not the case for Kuo (although clearly there is an indirect link through the creation of CAPE by moisture convergence.) Nevertheless the maintenance of large CAPE values emphasises a deficiency in the Kuo scheme. Fig.11 shows the results for Day 5 using the MM scheme and does represent instantaneous convective activity. The rather

'spotty' appearance does not result in 'spotty' accumulated precipitation as Fig.12 shows. The evolution of the global mean CAPE (the mean over all gridpoints with positive CAPE values) in two ten-day forecasts is shown in Fig.13 together with the number of points in the average. As can be seen, the MM scheme effects a rapid reduction to a mean value of about 160 J Kg^{-1} within 48 hrs, this value is undoubtedly more acceptable than a global mean of ~1000 J Kg^{-1} but there is a lack of direct radiosonde statistics to support these results. This rapid reduction to lower values is achieved primarily through the stabilizing effect of the downdraught fluxes into the boundary layer.

11.2 Global budget results

Since the global testing of the MM scheme is at a preliminary stage, the results given here will be restricted to some globally or zonally averaged comparisons. Global integrals of enthalpy (C_pT) and latent energy (Lq) and their sum are given in Fig.14. Although small fluctuations in these quantities might be expected, the systematic changes with time represent deficiencies in the model/analysis system. This is well known and occurs to some extent in all GCM's, but the principal interest here is in the effect of a different convective parametrisation scheme; also shown is the effect of enhancing the surface fluxes (as discused in Sect.10). The total thermodynamic energy (Fig.14a) decays much less rapidly through more vigorous energy input from the surface (increased by ~10%), a direct impact of the downdraught parametrisation in the MM scheme, with a further improvement in the enhanced case. Also evident in Fig.14b is the rapid heating and drying of the atmosphere in the early stages as excessive convective instability is removed.

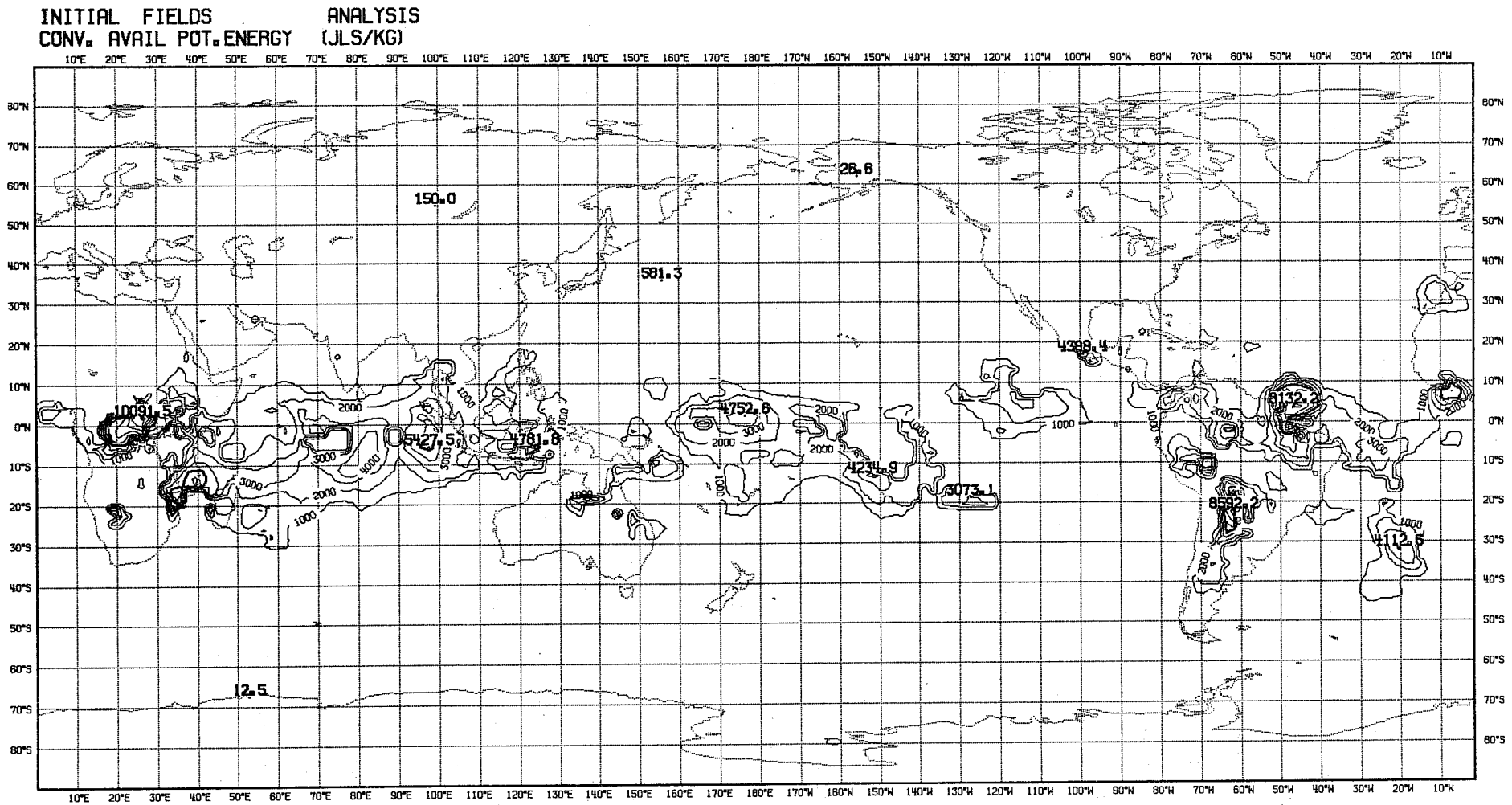

Fig. 8 The global distribution of convective available potential energy (CAPE) for FGGE analysis for 21/1/79. (contour interval = 1000 J/Kg).

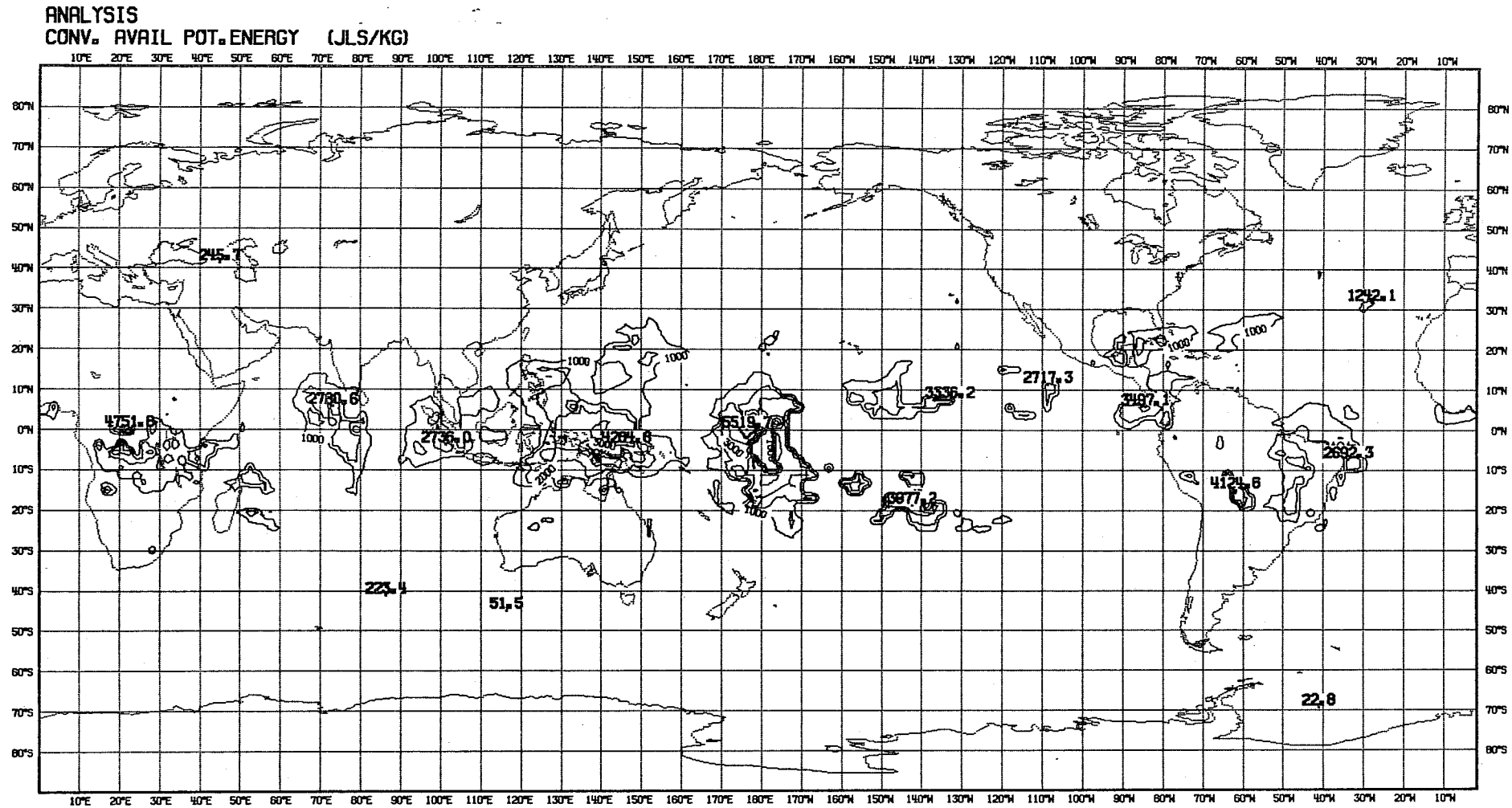

Fig. 9 As Fig. 8 but for 28/12/78 data re-analysed using improved analysis procedures.

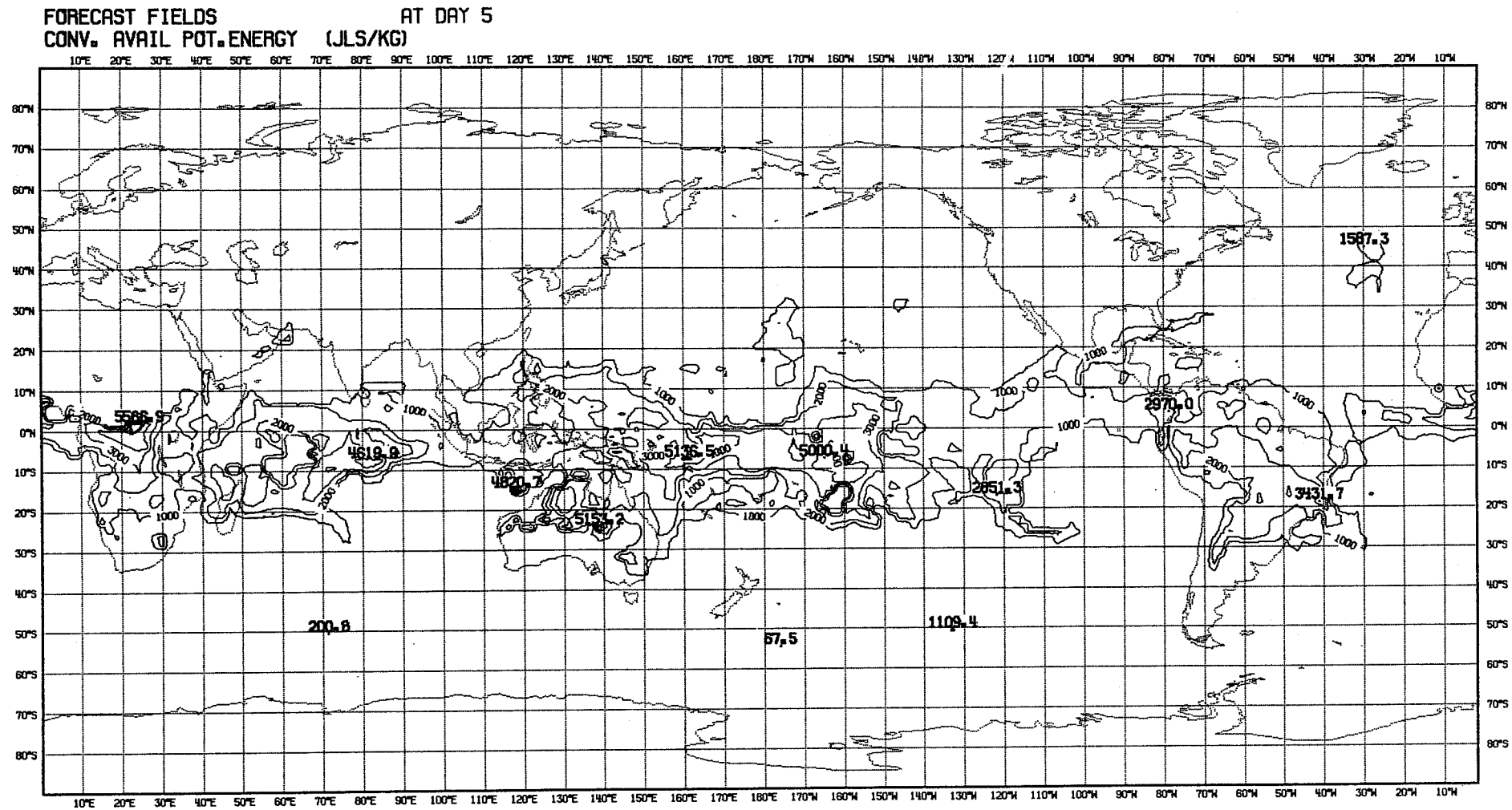

Fig. 10 As Fig. 8 but for the forecast fields at DAY 5 using the KUO scheme.

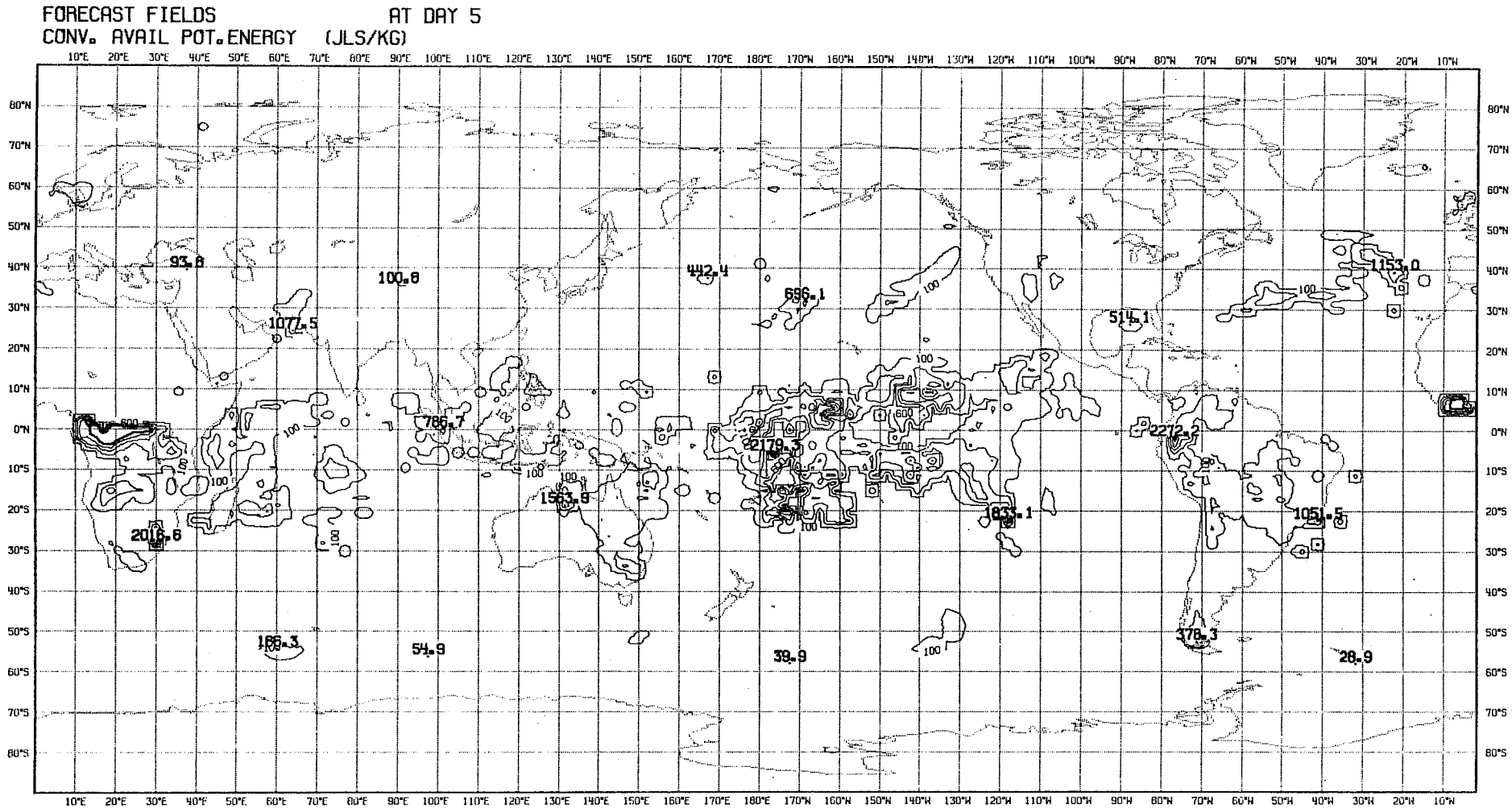

Fig. 11 As Fig. 10 but using the MM scheme. (N.B. Contour interval =500 J/Kg).

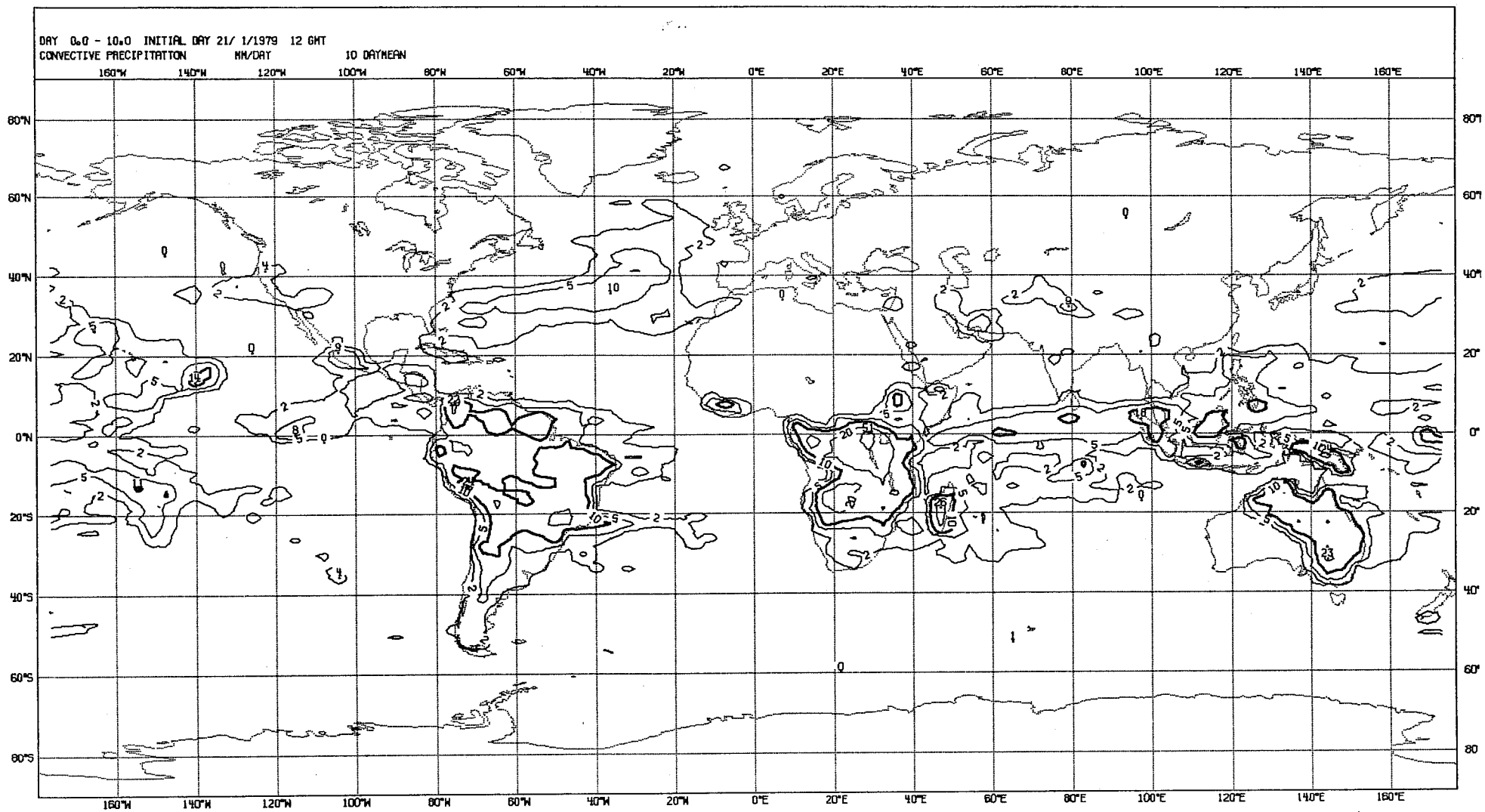

Fig. 12 The global convective rainfall distribution averaged over a 10-day Forecast from 21/1/79 data.

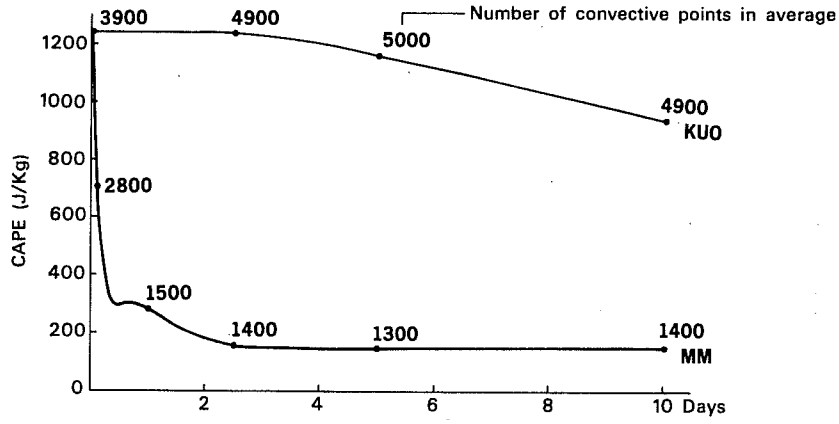

Fig. 13 The evolution of global mean CAPE for the two forecasts (KUO and MM). Also indicated are the number of grid points (with CAPE ≥ 0) contributing to the plotted mean.

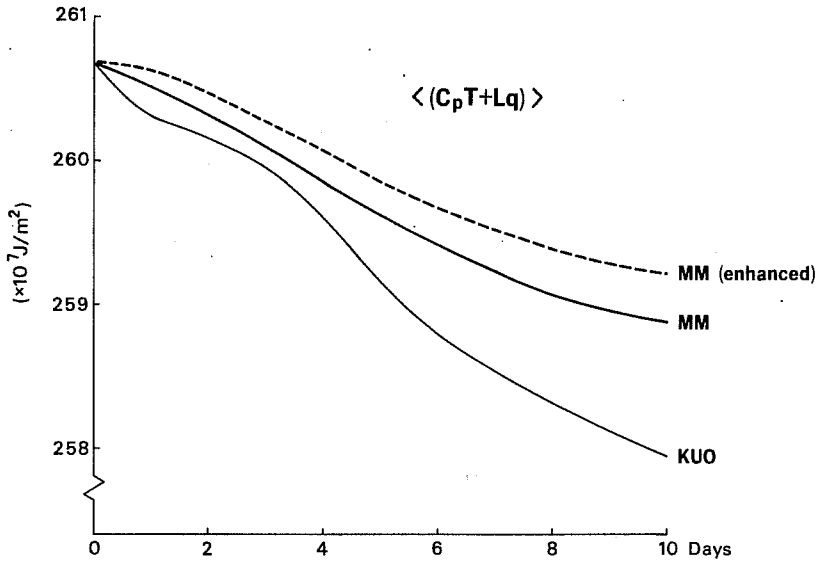

Fig. 14 a) The evolution of the globally averaged total thermodynamic energy $\langle\langle CpT+Lq \rangle\rangle$ for three forecasts, using the KUO and MM schemes and also with enhanced surfaces fluxes.

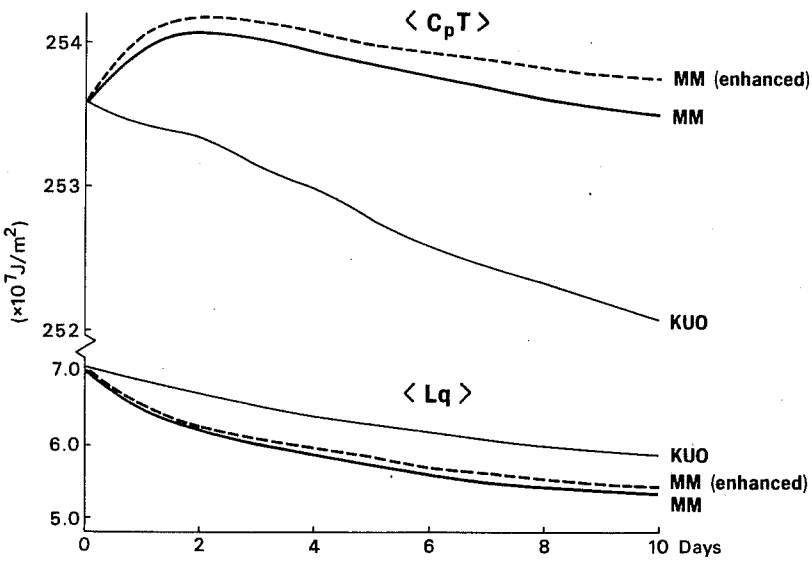

Fig. 14 b) As 14 a) but for the separate components.

In a 10 day forecast the major impact of the new convection scheme is seen in the tropics and in general the model errors are reduced in the later stages of the forecast with less tropospheric cooling and a reduction in zonal wind errors.

11.3 Forecast impact

As previously mentioned, the more detailed impact of the new convection scheme on medium-range forecasts (and on model climatology) is currently being studied. Initial results are encouraging, especially those with enhanced surface fluxes. The impact on higher latitudes of changes in the tropical circulations due to the new scheme and its momentum transports is significant but more work is needed in evaluating this, especially the response of the tropical atmosphere to direct dynamical forcing of the wind field.

12. CONCLUSIONS

This paper has established a theoretical basis for using dynamical cloud models in a parametrisation scheme for deep convection; this scheme has several novel features and results so far show it to be competitive with existing schemes. A number of different cloud models are identified with their implementation depending on grid-scale properties such as the vertical wind profile and CAPE which features strongly in the transport formulas. Global distributions of CAPE highlight analysis and model deficiencies and also provide a useful diagnostic for the physical processes in large-scale models. Downdraughts are an important entity in the cloud models and their transports are a natural part of the dynamical scheme, their interaction with the boundary layer by enhancing surface fluxes and rapidly modifying CAPE is significant and the results show that the representation of these processes may well be a strength of the new scheme. The scheme is able to represent

convective momentum transports in a dynamically consistent manner but the effect of these transports has yet to be properly tested.

Acknowledgements

The use and implementation of the above dynamical cloud models in the large-scale convective parametrisation scheme was developed in a joint project between Imperial College (Dr. M.J. Miller and Dr. M.W. Moncrieff) and the ECMWF Research Department. The use of ECMWF facilities and the cooperation of several research department staff are acknowledged. The basic dynamical research and analyses of the cloud models were undertaken at Imperial College, supported by NERC grants and studentships.

References

Arakawa, A. and Schubert, W. 1974: Interaction of a cumulus cloud ensemble with the large-scale environment: Part I. J.Atmos.Sci., 31, pp.674-701.

Browning, K.A. and Ludlam, F.H. 1962: Airflow in convective storms. Quart.J.R.Met.Soc., 88, pp.117-135.

Byers, H.R. and Braham, R.R. 1949: The Thunderstorm. US Govt.Print.Off., Washington, pp.287.

Fraedrich, K. 1973: On the parametrisation of cumulus convection by lateral mixing and compensating subsidence. J.Atmos.Sci., 30, pp.408-413.

Houze, R.A. 1977: Structure and dynamics of a tropical squall line system. Mon.Wea.Rev., 105, pp.1540-1567.

Houze, R.A. and Betts, A.K. 1981: Convection in GATE. Rev.Geophys.Space Phys., 19, pp.541-576.

Kuo, H.L 1974: Further studies of the influence of cumulus convection on large-scale flow. J.Atmos.Sci., 31, p.1232-1240.

Louis, J.-F., Tiedtke, M. and Geleyn, J.-F. 1982: A short history of the PBL parameterization at ECMWF. Workshop on planetary boundary layer parameterization in Nov.1981. ECMWF proceedings pp.59-81.

Ooyama, K. 1971: A theory of the parametrisation of cumulus convection. J.Met.Soc. Japan, 49, pp.744-756.

Marwitz, J.D. 1972: The structure and motion of severe storms: Parts I,II and III. J.Appl.Met., 11, pp.166-201.

Miller, M.J. 1978: The Hampstead storm; a numerical simulation of a quasi-stationary cumulonimbus. Ibid., 104, pp.351-365.

Moncrieff, M.W. 1978: The dynamical structure of two-dimensional steady convection in constant vertical shear. Quart.J.R.Met.Soc., 104, pp.543-567.

Moncrieff, M.W. 1981: A theory of the organised steady convection and its transport properties. Quart.J.Roy.Met.Soc., 107, pp.29-50.

Moncrieff, M.W. and Green, J.S.A. 1972: The propagation and transfer properties of two-dimensional steady convection in constant vertical shear. Quart.J.R.Met.Soc., 98, pp.336-353.

Moncrieff, M.W. and Miller, M.J. 1976: The dynamics and simulation of tropical sqall-lines. Ibid., 102, pp.373-394.

Newton, C.W. 1966: Circulations in large sheared cumulonimbus. Tellus, 18, pp.699-712.

Thompson, R.M., Payne, S.W., Recker, E.E. and Reed, R.J. 1979: Structure and properties of synoptic-scale wave disturbances in the intertropical convergence zone of the eastern Atlantic. J.Atmos.Sci., 36, pp.53-72.

Thorpe, A.J. Miller, M.J. and Moncrieff, M.W. 1980: Dynamical models of two-dimensional downdraughts. Quart.J.R.Met.Soc., 106, pp.463-485.

Thorpe, A.J. Miller, M.J. and Moncrieff, M.W. 1982: Two-dimensional convection in non-consistent shear: a model of mid-latitude squall lines. Ibid, 108, pp.739-762.

Zipser, E.J. 1969: The role of unsaturated convective downdrafts in the structure and rapid decay of an equatorial disturbance. J.Appl.Met., 8, pp.799-814.